HHS Public Access

Author manuscript

Cell Rep. Author manuscript; available in PMC 2024 November 16.

Published in final edited form as:

Cell Rep. 2024 October 22; 43(10): 114809. doi:10.1016/j.celrep.2024.114809.

The VLDLR entry receptor is required for the pathogenesis of multiple encephalitic alphaviruses

Sathvik Palakurty[1,2,8], **Saravanan Raju**[1,8], **Alan Sariol**[2,8], **Zhenlu Chong**[2], **Ngan Wagoner**[2], **Hongming Ma**[2], **Ofer Zimmerman**[2], **Lucas J. Adams**[1], **Camille Carmona**[2,3], **Zhuoming Liu**[3], **Daved H. Fremont**[1,3,4], **Sean P.J. Whelan**[3], **William B. Klimstra**[5], **Michael S. Diamond**[1,2,3,6,7,9,*]

[1]Department of Pathology & Immunology, Washington University School of Medicine, St. Louis, MO 63110, USA

[2]Department of Medicine, Washington University School of Medicine, St. Louis, MO 63110, USA

[3]Department of Molecular Microbiology, Washington University School of Medicine, St. Louis, MO 63110, USA

[4]Department of Biochemistry and Molecular Biophysics, Washington University School of Medicine, St. Louis, MO 63110, USA

[5]The Center for Vaccine Research and Department of Immunology, The University of Pittsburgh, Pittsburgh, PA 15261, USA

[6]Andrew M. and Jane M. Bursky Center for Human Immunology and Immunotherapy Programs, Washington University School of Medicine, St. Louis, MO 63110, USA

[7]Center for Vaccines and Immunity to Microbial Pathogens, Washington University School of Medicine, Saint Louis, MO 63110, USA

[8]These authors contributed equally

[9]Lead contact

SUMMARY

*Correspondence: mdiamond@wustl.edu.

AUTHOR CONTRIBUTIONS

S.P., S.R., and M.S.D. designed the study. S.P., S.R., O.Z., and Z.C. performed the screening, gene validation, and cell culture studies. C.C. generated key reagents used for some assays. S.R. and S.P. generated recombinant proteins and performed binding studies. A.S. and N.W. performed the infections in mice and virologic analysis. H.M., Z.L., and S.P.J.W. contributed to development of the CRISPR library in Hap1 cells. L.J.A. and D.H.F. supervised the protein binding studies. W.B.K. and M.S.D. secured funding and resources for the studies. S.P., S.R., and M.S.D. wrote the initial draft, with all other authors providing comments.

DECLARATION OF INTERESTS

M.S.D. is a consultant to or on the scientific advisory board for Inbios, IntegerBio, Akagera Medicines, Merck, GlaxoSmithKline, and Moderna. The Diamond laboratory has received unrelated funding support in sponsored research agreements from Emergent BioSolutions, Moderna, IntegerBio, and Vir Biotechnology. D.H.F. is a founder of Courier Therapeutics and has received unrelated funding support from Emergent BioSolutions and Mallinckrodt Pharmaceuticals.

SUPPLEMENTAL INFORMATION

Supplemental information can be found online at https://doi.org/10.1016/j.celrep.2024.114809.

The very-low-density lipoprotein receptor (VLDLR) has been reported as an entry receptor for Semliki Forest (SFV) and Eastern equine encephalitis (EEEV) alphaviruses in cell cultures. However, the role of VLDLR in alphavirus pathogenesis and the extent to which other alphaviruses can engage VLDLR remains unclear. Here, using a surface protein-targeted CRISPR-Cas9 screen, we identify VLDLR as a receptor for Western equine encephalitis virus (WEEV) and demonstrate that it promotes the infection of multiple viruses in the WEE antigenic complex. *In vivo* studies show that the pathogenicity of WEEV, EEEV, and SFV, but not the distantly related Venezuelan equine encephalitis virus, is markedly diminished in VLDLR-deficient mice and that mice treated with a soluble VLDLR-Fc decoy molecule are protected against disease. Overall, these results expand our understanding of the role of VLDLR in alphavirus pathogenesis and provide a potential path for developing countermeasures against alphaviruses from different antigenic complexes.

Graphical Abstract

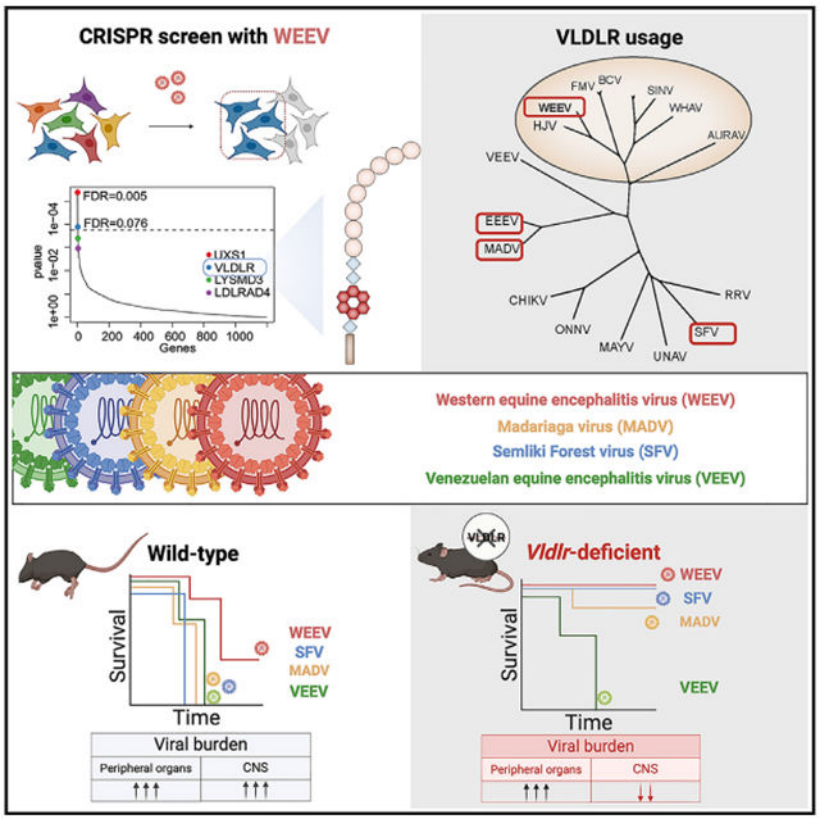

In brief

Using a targeted CRISPR-Cas9 survival screen, Palakurty et al. identify the very-low-density lipoprotein receptor (VLDLR) as a receptor for Western equine encephalitis virus (WEEV) and other related viruses in its antigenic complex. Their experiments also demonstrate that the pathogenesis of multiple encephalitic alphaviruses is substantially reduced in VLDLR-deficient mice.

INTRODUCTION

Alphaviruses are arthropod-transmitted, enveloped, positive-strand RNA viruses that cause musculoskeletal disease orencephalitis in humans. The encephalitic alphaviruses are classified in three antigenically defined serocomplexes (Figure 1A) and include Eastern equine encephalitis virus (EEEV), Venezuelan equine encephalitis virus (VEEV), and Western equine encephalitis virus (WEEV), each of which can cause severe neurological syndromes in humans and horses resulting in long-term sequelae or death.[1-4]

The WEE serocomplex is comprised of several related viruses, including WEEV, Sindbis virus (SINV), Ockelbo virus (OCKV), Babanki virus (BBKV), Aura virus (AURV), Buggy Creek virus (BCV), and Highlands J virus (HJV). An ancestral alphavirus derived from a recombination event of the E2 and E1 genes from a SINV-like virus and the capsid, nonstructural genes, and RNA replication control sequences of an antecedent EEEV strain diversified and evolved into the WEEV, BCV, and HJV. Birds and mosquitoes serve as the enzootic reservoir for WEEV, horses serve as an epizootic amplifying host, and humans are infected but do not sustain sufficient viremia for transmission.[5] Although human WEEV infections remain rare, the potential for their emergence due to the spread or adaptation of mosquito vectors or bioweaponization highlights a need for a greater understanding of its biology and the development of preventative or therapeutic measures. Indeed, an epizootic outbreak of WEEV infection in horses in Argentina in early 2024 has caused fatal human and equine cases.[6] Although no approved countermeasures exist for WEEV or other encephalitic alphaviruses, a virus-like particle (VLP)-based trivalent vaccine elicited neutralizing antibodies in a phase 1 trial.[7]

Several entry receptors have recently been described for arthritogenic and encephalitic alphaviruses including mammalian MXRA8 (for chikungunya virus [CHIKV], Ross River virus [RRV], Mayaro virus [MAYV], and O'nyong'nyong virus [ONNV]), LDLRAD3 (exclusively for VEEV), very-low-density lipoprotein receptor (VLDLR; for EEEV, Semliki Forest virus [SFV], and, to a lesser degree, SINV), ApoER2 (for EEEV, SFV, and SINV), and LDLR (for EEEV, WEEV, SFV, and Getah virus).[8-12] In addition, the avian ortholog of MXRA8 was identified as a receptor for SINV, WEEV, and other members of the WEE serocomplex.[13] For WEEV, although infection of cells was reduced when LDLR expression was abrogated, substantial residual infection was apparent, suggesting the existence of additional, and possibly more dominant, mammalian entry receptors.[12]

Here, we perform a CRISPR-Cas9 loss-of-function cell survival screen in human haploid HAP1 cells and identify VLDLR as an entry factor for multiple strains of WEEV. Expression of VLDLR on cells enhances binding to and internalization of WEEV, and biolayer interferometry experiments confirm a direct interaction between the ligand-binding domain (LBD) of VLDLR and WEEV virions. Based on these data, we generated a soluble VLDLR-LBD-Fc decoy molecule that neutralizes WEEV infection in cell culture and protects against disease in mice. Consistent with these results, the pathogenesis of several encephalitic alphaviruses that utilize VLDLR, including SFV, EEEV (Madariaga virus strain [MADV]), and WEEV, is reduced in VLDLR-deficient mice. Overall, our experiments

establish a physiologically important role for VLDLR as an entry factor for WEEV and other encephalitic alphaviruses that interact with this receptor.

RESULTS

A CRISPR-Cas9 screen identifies VLDLR as factor that promotes WEEV infection

To identify possible entry factors for WEEV, we used a CRISPR-Cas9 loss-of-expression screening approach with a custom-made library of 4,630 single guide RNA (sgRNA) targeting 1,146 genes (~4 sgRNAs per gene) predicted to have cell surface expression, along with 50 non-targeting guides to serve as controls (Table S1). This surface protein-targeting (hereafter, Surfaceome) library was introduced by lentiviral transduction into human HAP1 leukemia cells, a haploid line that facilitates penetrance of Cas9-mediated gene editing. We then inoculated Surfaceome library-transduced HAP1 cells with SINV-WEEV-GFP McMillan, a chimeric virus that encodes the nonstructural genes (nsp1–nsp4) of SINV, a green-fluorescent reporter protein (GFP), and the structural genes (C-E3-E2-6K-E1) of WEEV (McMillan strain), enabling the screen to be performed under lower biosafety containment (i.e., BSL2 instead of BSL3) conditions. Greater than 99% of infected HAP1 cells died within 5 days of SINV-WEEV-GFP McMillan infection. The few surviving cells were recovered, propagated, and subjected to a second round of SINV-WEEV-GFP McMillan infection (Figure S1A). Surviving cells were harvested and sequenced to assess for gRNA enrichment. The screen revealed two significantly enriched genes (false discovery rate [FDR] < 0.1): *Uxs1,* a protein involved in glycosaminoglycan (GAG) synthesis, and *VLDLR* (Figure 1B; Table S2).

Given that VLDLR was identified as a receptor for EEEV and SFV,[10] we focused on validating its effect on WEEV infection. We generated *ΔVLDLR* HAP1 cells using CRISPR-Cas9 gene editing along with a control, non-targeting guide-expressing cell line (Figure S1B). Loss of VLDLR expression resulted in a decrease in infection with SINV-WEEV-GFP McMillan, which was restored by complementation with an N-terminally FLAG-tagged VLDLR (Figures 1C and S1C). Moreover, SINV-WEEV-GFP McMillan infection in parental HAP1 cells was reduced by treating cells with an anti-VLDLR antibody (Figures 1D and S1D) to a level like that observed in Δ*VLDLR* HAP1 cells. The partial reduction in infection of HAP1 cells conferred by the loss of VLDLR expression or antibody blockade suggests the presence of additional entry factor(s) that can promote infection.

VLDLR expression supports infection of multiple WEE complex members

We next tested whether ectopic expression of VLDLR could promote WEEV infection in K562 erythroleukemic cells, which show limited permissiveness to many alphaviruses due to entry-stage defects.[10,14] As controls and for comparison, we expressed chicken or mouse MXRA8 in K562 cells: chicken MXRA8 promotes infection of many WEE complex viruses, whereas mouse MXRA8 enables infection of arthritogenic alphaviruses including CHIKV, MAYV, and RRV.[8,13] Ectopic expression of VLDLR or chicken MXRA8 supported infection of SINV-WEEV-GFP McMillan but not RRV (Figures 1E, S2A, and S2B). We confirmed these results with infectious clone-derived, authentic WEEV McMillan (Figure 1F). Expression of VLDLR in K562 cells supported infection of other chimeric

SINV-WEEV-GFP viruses encoding the structural genes of WEEV Fleming or 71V-1658 but not those of WEEV CBA87, Imperial 181, or BFS2005. VLDLR expression also did not support infection of a chimeric WEEV in which the structural genes of WEEV McMillan were replaced with those of a strain (EQ1090_2023) from the recent outbreak in Argentina (Figures 1G-1I). We next assessed whether VLDLR could enhance the infection of other alphaviruses in the WEE complex (Figure 1A). Indeed, expression of VLDLR in K562 cells promoted the infection of BBKV, OCKV, BCV, and SINV (Figures 1J and S2C). Thus, VLDLR can promote infection of some WEEV strains and multiple WEE complex family members.

To extend our results, we performed multi-step growth analysis with SINV-WEEV McMillan, SINV-EEEV FL93-939, and RRV T48 in K562 cells expressing VLDLR, chicken MXRA8, or mouse MXRA8 (Figure 1K). Expression of VLDLR enhanced SINV-WEEV and SINV-EEEV yields in the supernatant compared to control K562 or K562 cells expressing mouse MXRA8. Reciprocally, expression of mouse MXRA8 enhanced RRV, but not SINV-WEEV or SINV-EEEV, infection.

The LBD of VLDLR promotes WEEV binding and internalization

We next determined whether VLDLR promoted WEEV entry by performing cell binding and internalization assays on control, VLDLR-expressing, and chicken MXRA8-expressing K562 cells. To assess attachment, the virus was incubated with cells at 4°C, and after extensive washing to remove unbound virus, binding to intact cells was measured by flow cytometry using an anti-WEEV E2 monoclonal antibody (mAb). Compared to control K562 cells, expression of VLDLR or chicken MXRA8 enhanced the binding of SINV-WEEV McMillan virions (Figures 2A and 2B). When virus and cells were incubated at 37°C for 1 h, greater amounts of intracellular SINV-WEEV were detected in VLDLR- and chicken MXRA8-expressing cells, as determined by antigen staining and flow cytometry after treating the cells with proteinase K, which degrades surface-bound but not internalized virus (Figures 2C and 2D). These results confirm that expression of VLDLR enhances the cellular entry of WEEV virions.

The ectodomain of VLDLR is comprised of 8 LDLR type A (LA) domains (the LBD), 3 epidermal growth factor (EGF)-like domains, and a beta-propeller domain (Figure 2E). As seen with EEEV and SFV,[10] deletion of the LBD of VLDLR abrogated SINV-WEEV-GFP McMillan infection, suggesting that the LBD is critical for its interaction (Figure 2E). In contrast, the transmembrane and cytoplasmic domains of VLDLR were dispensable for SINV-WEEV-GFP McMillan binding, internalization, and infection of K562 cells (Figures S2E-S2I), as we observed previously for MXRA8 and LDLRAD3 interactions with CHIKV and VEEV, respectively.[8,9] To confirm this result, we expressed and purified soluble VLDLR-LBD-Fc (human Fc) protein and assessed its binding to the surface of infected Vero cells that display the alphavirus E1/E2 structural proteins (Figure S3A). VLDLR-LBD-Fc bound to the surface of SINV-WEEV McMillan and SINV-EEEV FL93-infected cells in a concentration-dependent manner (Figures 2F and S3B) but not to SINV-VEEV Trinidad donkey (TrD)- or SINV-CHIKV La Reunion 2006 (LR)-infected cells. As controls, LDLRAD3-LA1-Fc, which contains the LDLRAD3 binding domain of VEEV,

and mouse MXRA8-Fc only bound to the surface of SINV-VEEV TrD- and SINV-CHIKV LR-infected cells, respectively (Figures 2F and S3B). We next assessed whether VLDLR-LBD-Fc could interact directly with WEEV VLPs (Figure S3C), which are structurally identical to mature virions.[13] We captured WEEV McMillan, VEEV TC-83, or CHIKV 37997 VLPs on biosensors using mouse anti-alphavirus mAbs and then added VLDLR-LBD-Fc, LDLRAD3-LA1-Fc, or mouse MXRA8-Fc. As expected, VEEV VLPs bound to LDLRAD3-LA1-Fc but not to VLDLR-LBD-Fc or mouse MXRA8-Fc, whereas CHIKV VLPs bound to mouse MXRA8-Fc but not to VLDLR-LBD-Fc or LDLRAD3-LA1-Fc (Figure 2G, left). In comparison, WEEV McMillan VLPs bound to VLDLR-LBD-Fc but not to LDLRAD3-LA1-Fc or mouse MXRA8-Fc (Figure 2G, right).

Neutralization with VLDLR-LBD-Fc decoy molecules

Given the direct binding of VLDLR-LBD-Fc to WEEV McMillan VLPs in solution, we hypothesized that this decoy receptor could inhibit WEEV infection. To test this idea, we mixed increasing concentrations of VLDLR-LBD-Fc or LDLRAD3-LA1-Fc with SINV-WEEV-GFP McMillan or SINV-VEEV-GFP TrD before adding the complexes to HEK293T cells. The cells were harvested, and infection levels were determined by flow cytometry. Whereas SINV-WEEV-GFP McMillan infection was neutralized potently by VLDLR-LBD-Fc (half-maximal inhibitory concentration [EC_{50}] ~20 ng/mL), SINV-VEEV-GFP TrD infection was not inhibited by VLDLR-LBD-Fc (Figures 3A and S4A). Reciprocally, incubation of SINV-VEEV-GFP TrD, but not SINV-WEEV-GFP McMillan, with LDLRAD3-LA1-Fc resulted in efficient inhibition of infection (Figure 3A). Because WEEV infects multiple vertebrate animal species in its enzootic and epizootic cycles, including birds and horses, we tested whether orthologous VLDLR decoy molecules also could inhibit SINV-WEEV-GFP McMillan infection. Recombinantly expressed VLDLR-LBD-Fc proteins derived from birds (sparrow and starling) or horse VLDLR efficiently neutralized SINV-WEEV-GFP McMillan infection in HEK293T cells (Figure S4B). We also evaluated if VLDLR-LBD-Fc could obscure heterologous receptor-binding sites and prevent cellular entry of WEEV mediated by avian MXRA8. We inoculated VLDLR- or chicken MXRA8-expressing K562 cells with SINV-WEEV virions that had been pre-mixed with VLDLR-LBD-Fc. Notably, SINV-WEEV-GFP McMillan infection of K562-VLDLR and K562-chicken MXRA8 cells was inhibited equivalently across a range of doses of VLDLR-LBD-Fc (Figure 3B). These results suggest that the binding sites of VLDLR and avian MXRA8[13] on WEEV are proximally located.

VLDLR-LBD-Fc soluble decoy protects mice against WEEV infection

To begin to define possible countermeasures for WEEV and confirm the importance of VLDLR as a receptor for WEEV, we first evaluated whether co-administration of virus with VLDLR-LBD-Fc via the same subcutaneous injection route could protect wild-type C57BL/6J mice from pathogenic WEEV-McMillan infection. Weight loss and mortality observed after WEEV infection were diminished markedly by treatment with VLDLR-LBD-Fc compared to the LDLRAD3-LA1-Fc control protein (Figure 3C). At 4 days post-infection (dpi), we also observed lower levels of WEEV RNA in the brain, kidney, and spleen of animals treated with VLDLR-LBD-Fc than LDLRAD3-LA1-Fc (Figure 3D). As a control, we administered VLDLR LBD-Fc and LDLRAD3-LA1-Fc to C57BL/6J mice prior

to infection with a virulent VEEV ZPC738 strain. Mice administered LDLRAD3-LA1-Fc were protected from weight loss and death, whereas those given VLDLR-LBD-Fc were not (Figure 3E). As an additional test, we administered VLDLR-LBD-Fc or LDLRAD3-LA1-Fc protein separately by intraperitoneal injection and subsequently inoculated mice with WEEV McMillan by subcutaneous inoculation. VLDLR-LBD-Fc-treated mice had lower viral titers in the brain, kidney, and spleen than LDLRAD3-LA1-Fc-treated animals (Figure 3F).

VLDLR is required for the pathogenesis of WEEV, SFV, and EEEV

Although our cell culture and inhibitory receptor decoy experiments strongly support a role for VLDLR in WEEV entry and infection, the significance of this interaction *in vivo* for pathogenesis remained uncertain. To address this question, we obtained commercially available *Vldlr*$^{-/-}$ mice on a mixed C57BL6/129 background along with wild-type C57BL6/J, 129SvJ, and B6129SF2/J (B6/129) control mice. We inoculated age- and sex-matched mice with $10^{3\backslash}$ focus-forming units (FFUs) of WEEV McMillan and monitored weight loss and survival. All C57BL6/J mice succumbed to WEEV infection by 6 dpi, whereas the 129Sv/J and B6/129 mice sustained 50% mortality rates (Figure 4A). In comparison, after WEEV infection, all *Vldlr*$^{-/-}$ mice survived (Figure 4A). These results suggest that VLDLR is a key host factor required for WEEV pathogenesis.

We also tested whether VLDLR is important for the pathogenesis of other encephalitic alphaviruses. In a first set of experiments, we inoculated C57BL6/J, B6/129, and *Vldlr*$^{-/-}$ mice with 10^3 FFUs of SFV (Kumba strain) via intraperitoneal injection. Whereas C57BL6/J and B6/129 mice succumbed to SFV infection within 7 days, *Vldlr*$^{-/-}$ mice were protected (Figure 4B). We next evaluated the role of VLDLR in EEEV pathogenesis by inoculating C57BL6/J, 129SvJ, B6/129, and *Vldlr*$^{-/-}$ mice with 2×10^2 FFUs of EEEV-MADV (Argentina 1936 strain), a South American EEEV lineage that lacks Select Agent designation and can use VLDLR as an entry factor (Figure S4C). Whereas most (90%) B6/129 mice succumbed to EEEV-MADV infection, *Vldlr*$^{-/-}$ mice sustained reduced lethality (Figure 4C). Finally, a deficiency of VLDLR did not impact the pathogenesis of VEEV, which uses LDLRAD3, but not VLDLR, as an entry receptor[9,15]; all wild-type and *Vldlr*$^{-/-}$ mice inoculated with 10^2 FFUs of VEEV ZPC738 succumbed to infection with equivalent kinetics (Figure 4D). These results establish a critical role for VLDLR in mediating the pathogenesis of WEEV, SFV, and EEEV in mice.

To extend these findings, we examined how a deficiency of VLDLR impacted WEEV burden in tissues at 5 dpi. In comparison to control B6/129 mice, which exhibited high viral burden in the brain, *Vldlr*$^{-/-}$ mice showed markedly reduced WEEV RNA levels (~10,000-fold, $p < 0.0001$), consistent with the improved survival phenotype in *Vldlr*$^{-/-}$ mice and the expression pattern of *Vldlr* in both oligodendrocytes and neurons of the mouse brain (Figures 4E and S5). However, and in contrast to that seen with VLDLR LBD-Fc (Figure 3E), the kidney and spleen did not show significant differences in WEEV infection in control and *Vldlr*$^{-/-}$ mice (Figure 4E), suggesting a possible subordinate role for VLDLR outside of the brain. Given these results, we next tested directly whether the VLDLR had an intrinsic role in WEEV infection in the brain by performing intracranial inoculation experiments. Compared to control mice, at 36 h post-infection, *Vldlr*$^{-/-}$ mice

had significantly reduced viral infection in the cortex (15-fold, $p < 0.01$), cerebellum (121-fold, $p < 0.01$), and brain-stem (39-fold, $p < 0.01$) (Figure 4F).

DISCUSSION

Viruses must engage cell surface molecules to enter and infect host cells. This key interaction is critical in viral tropism, virulence, and species restriction. Here, using a CRISPR-Cas9 loss-of-function screen in HAP-1 cells, we identified VLDLR as a receptor for WEEV and other members of the WEE complex of alphaviruses, thus extending its use beyond that reported for SFV, EEEV, and possibly SINV.[10] Moreover, our *in vivo* studies with VLDLR-deficient mice establish a key role for VLDLR in the pathogenesis of WEEV and other alphaviruses, including SFV and EEEV but not VEEV.

Although our loss-of-function genetic screen identified *VLDLR* as a factor promoting resistance to WEEV infection and cell death, experiments in *ΔVLDLR* cells or with blocking anti-VLDLR antibodies revealed a partial phenotype, with residual WEEV infection observed. Analogously, WEEV infection was detected in *Vldlr*$^{-/-}$ mice, albeit at lower levels, especially in the brain. We speculate that in the absence of VLDLR, alternative receptors might compensate and enable WEEV infection; indeed, we recently identified the related LA-domain-containing molecule LDLR as an entry factor for WEEV on neuronal cells.[12] Our HAP1 cell CRISPR-Cas9 survival screen also identified *UXS1* as a statistically significant “hit.” UXS1 catalyzes the synthesis of UDP-xylose, which is required for the generation of GAGs, including heparan and chondroitin sulfates. Consistent with our screening result, GAGs have been identified as key attachment moieties and possible receptors for several alphaviruses in cell culture.[16-20] This observation of multiple receptor entry pathways for alphaviruses may be a more general paradigm, as in all cases to date, infection has been demonstrated even in the absence of expression of a dominant receptor (e.g., MXRA8 for CHIKV, LDLRAD3 for VEEV, and VLDLR for EEEV).[8-10] Consistent with this idea, a recent CRISPR-based screen identified the protocadherin PCDH10 as a receptor for several WEEV strains[21]; it remains to be tested whether this molecule explains the residual VLDLR-independent infection by WEEV in mice and some human cells. The use of VLDLR by WEEV might have been predicted since SINV, a member of the WEE antigenic complex, shares ~70% identity of its structural proteins with WEEV and was shown to use VLDLR to some extent.[10] However, the levels of SINV infection supported by VLDLR in our K562 cells appear lower than some of the WEEV strains we tested. During the writing of our paper, a study was published that used reporter virus particles (RVPs) to identify VLDLR as a receptor for a subset of WEEV strains, including WEEV McMillan and WEEV Fleming.[21] Their experiments, however, showed little infection of WEEV CBA87, Imperial 181, and 71V-1658 RVPs in K562-VLDLR cells, which agrees with our findings with several fully infectious SINV-WEEV strains. One difference we observed is a low but detectable level of SINV-WEEV 71V-1658 infection, which could be due to variation in VLDLR expression level on K562 cells between groups or the multiple rounds of infection in our experimental system. Although structural characterization is required, variation in key contact residues in the E1 and/or E2 protein could explain the variation in VLDLR-mediated infection between WEEV strains, SINV, and other alphaviruses.

Our studies in mice establish that VLDLR has an important role in the pathogenesis of WEEV, SFV, and EEEV. These data resemble the attenuated VEEV infection phenotype observed in LDLRAD3-deficient mice,[9,15] which showed a dominant contribution of LDLRAD3 to VEEV pathogenesis. While *Vldlr*$^{-/-}$ mice did not succumb to WEEV- or SFV-infection-induced lethality, partial lethality was observed after EEEV-MADV infection. This result suggests that other entry factors, possibly LDLR and/or ApoER2,[10,12] contribute to the pathogenesis of EEEV-MADV in mice. Along these lines, while we observed WEEV RNA in the brain of *Vldlr*$^{-/-}$ mice after subcutaneous virus inoculation, this lower level of infection was not sufficient to cause severe pathogenesis. Additional studies will be needed to delineate the cellular and tissue contexts in which alternative WEEV receptors are utilized *in vivo.* Finally, as decreased viral burden was measured in the brain of *Vldlr*$^{-/-}$ mice after intracranial virus inoculation, there likely is an intrinsic role of VLDLR for WEEV entry and infection in the central nervous system.

We previously leveraged the distinct binding modes of mammalian and avian MXRA8 for CHIKV and WEEV to generate a chimeric MXRA8-Fc decoy protein. This molecule neutralized CHIKV and WEEV *in vitro* and conferred protection *in vivo* against both viruses in mice.[13] In our current study, we observed that VLDLR-LBD-Fc also protected against WEEV-induced lethality in mice, similar to our prior study with VLDLR-derived decoy molecules and EEEV.[14] Given these findings, the development of bispecific MXRA8- and VLDLR-based fusion proteins might be a path to developing a pan-alphavirus decoy molecule. Future work will be needed to establish the minimal domains of VLDLR LBD-Fc required for inhibitory activity against WEEV to improve pharmacokinetic properties.

Limitations of the study

While our data support a role for VLDLR in the entry of WEEV in mammalian cells and for pathogenesis in a mouse model, we acknowledge several limitations in our study. (1) It is undefined when and how WEEV virions are released from VLDLR to enable penetration from the endosome into the cytosol or what other host factors contribute to this process. (2) Our *in vivo* data have not established which key cell types show VLDLR dependence for WEEV infection and pathogenesis. The use of conditional knockout mice could address this question. (3) The delineation of the exact LA domain(s) within VLDLR and the corresponding residues on the viral glycoproteins that mediate this interaction could provide insight as to how VLDLR can engage multiple distantly related alphaviruses and why it supports the infection of only some WEEV strains. (4) Optimization of the biodistribution of VLDLR-Fc decoy molecules (either full-length or a subset of domains) will be required for possible development as therapeutics. (5) All of our *in vivo* studies utilize WEEV McMillan for infection and thus require confirmation with other WEEV strains that engage VLDLR.

In summary, our experiments showing that VLDLR promotes the infection of several WEEV strains and WEE complex members extends our understanding of alphavirus receptor biology and the contribution of this receptor to pathogenesis. Future studies will be aimed at determining the structural basis of WEEV-VLDLR binding, identifying additional WEE complex receptors that explain the residual infection in *Vldlr*$^{-/-}$ cells, and generating

improved decoy or small molecules that broadly inhibit virus-receptor engagement of multiple alphaviruses from different antigenic complexes.

RESOURCE AVAILABILITY

Lead contact

Further information and requests for resources and reagents should be directed to the lead contact, Michael S. Diamond (mdiamond@wustl.edu).

Materials availability

All requests for resources and reagents should be directed to the lead contact. This includes viruses, primer-probe sets, and mice. All reagents will be made available upon request after completion of a materials transfer agreement (MTA).

Data and code availability

All data supporting the findings of this study are available within the paper or from the corresponding author upon request. This paper does not include original code. Any additional information required to reanalyze the data reported in this paper is available from the lead contact upon request.

STAR★METHODS

EXPERIMENTAL MODEL AND STUDY PARTICIPANT DETAILS

Cells—HEK293T (ATCC, CRL-3216), Vero (ATCC, CCL-81), and BHK21 (ATCC, CCL-10) cells were propagated in high-glucose Dulbecco's Modified Eagle Media (DMEM) supplemented with 10% FBS, Gluta-MAX, 10 mM HEPES, non-essential amino acids, and penicillin-streptomycin. K562 cells (ATCC, CCL-243) were maintained in RPMI-1640 (Thermo Fisher) supplemented with 10% FBS, Gluta-MAX, 10 mM HEPES, and penicillin-streptomycin. HAP1 (Horizon Discovery, C631) cells were maintained in Iscove's Modified Dulbecco Media (IMDM) supplemented with 10% FBS, Gluta-MAX, 10 mM HEPES, non-essential amino acids, and penicillin-streptomycin.

Mice—C57BL/6J (Cat #000664), 129S1/SvImJ (Cat #002448), B6129SF2/J (B6/129; Cat # 101045), and *Vldlr*$^{-/-}$ (Cat # 002529) were purchased from Jackson Laboratories and maintained in a specific-pathogen-free facility. Six-to nine-week-old male and female mice were used in all experiments. Experimental procedures were approved by the Washington University School of Medicine Institutional Animal Care and Use Committee (assurance number A3381-01) and followed the guidelines of the Guide for the Care and Use of Laboratory Animals. Virus inoculations were performed under anesthesia induced by ketamine hydrochloride and xylazine.

Viruses—WEEV McMillan and VEEV ZPC738 were generated from infectious cDNA clones as described[22,23] with the McMillan cDNA modified as described.[24] SFV (Kumba strain), EEEV-MADV (Argentina 1936 strain), BBKV (DAK ArY 251), OCKV (EDS 14), BCV (84S217 strain), and SINV (Toto) were obtained from the World Reference Center

for Emerging Viruses and Arboviruses (University of Texas Medical Branch, generous gift of Scott Weaver and Kenneth Plante). SINV Girdwood was a gift from Mark Heise (Geise Chapel Hill, NC). All viruses were propagated in BHK-21 cells and titered by focus-forming assay on Vero cells.

The SINV-WEEV-GFP McMillan and SINV-WEEV McMillan infectious clones were described previously.[25] The cDNA encoding the structural genes of WEEV Fleming (MN477208.1), WEEV 71V-1658 (NC003908.1), BFS2005 (GQ287644.1), CBA87 (DQ432026.1), Imperial 181 (GQ287641.1), and EQ1090_2023 (PP544260.1) were synthesized and cloned into the pCMV vector by Twist Biosciences. The SINV-WEEV-GFP 71V-1658, SINV-WEEV-GFP Fleming, SINV-WEEV-GFP BFS2005, SINV-WEEV-GFP CBA87, and SINV-WEEV-GFP Imperial 181 infectious cDNA clones were generated by PCR of the structural genes and subsequent Gibson assembly. A chimeric virus with the non-structural genes of WEEV McMillan and the structural genes of EQ1090_2023 was generated by gene synthesis and Gibson assembly. RRV T48-GFP was generated from the pRR64-GFP infectious clone[26,27] as described below.

METHOD DETAILS

Generation of viruses—To generate viruses from infectious clones, DNA was linearized by restriction digestion and purified using the Monarch PCR & DNA Clean up Kit (New England BioLabs). Subsequently, 1 μg of linearized vector was used as a template for genomic RNA synthesis using the HiScribe SP6 RNA synthesis kit (New England BioLabs) followed by purification using the Monarch RNA clean up kit. For high titer growth of some WEEV strains, we transduced BHK21 cells with a lentivirus encoding N-terminal FLAG tagged chicken (c)MXRA8 cloned into pLV-Blast vector. BHK21 cells or BHK21-cMXRA8 cells were transfected with 4 μg of the resulting RNA using a GenePulser Xcell electroporator with a 2mm cuvette (Voltage = 850 V, resistance = 25 μF, resistance = ◦ Ω). After 48 to 72 h h, the supernatant was collected as the P0 stock and passaged one additional time on BHK21 or BHK21-cMXRA8 cells; this P1 stock was titered on Vero cells by focus-forming assay and used for all subsequent experiments. To verify the sequence of the P1 stock, RNA was extracted from the viral supernatant with a MagMax Viral RNA isolation kit according to the manufacturer protocol using a Kingfisher Flex instrument. cDNA was synthesized using ProtoScript II cDNA synthesis kit (NEB) with random hexamers according to manufacturer's instructions. The structural genes were amplified, and the PCR product was purified with the ChargeSwitch PCR purification kit (Thermo Fisher) according to manufacturer protocol and subjected to long-read amplicon sequencing using the Oxford Nanopore platform by Plasmidsaurus (Eugene, OR).

Phylogenetic analysis—The E1 and E2 protein sequences CHIKV (QKY67868.1), MAYV (QED21311.1), Una (UNAV, YP_009665989.1), ONNV (AAC97205.1), SFV (NP_463458.1), RRV (AAA47404.1), EEEV (ANB41743.1), EEEV-MADV, AXV43855.1), VEEV (AGE98294.2), SINV (AAM10630.1), AURAV (NP_632024.1), OCKV (P27285.1), WEEV (QEX51909.1), Buggy Creek virus (BCV, AEJ36227.1), BBKV (AVN98166.1), FMV (YP_003324588.1), HJV (YP_002802300.1), and WHAV (AEJ36239.1) were obtained from NCBI GenBank. Clustal Omega was used to align the sequences with simple

phylogeny inferred via neighbor-joining.[28] Results were visualized in R using the ggtree package.[29]

CRISPR-Cas9 sgRNA library design, screening, and analysis—A list of 1,146 surface proteins was obtained based on datasets for plasma membrane proteins.[30] Four sgRNAs targeting each gene were picked genome-wide Brunello CRISPR-KO library,[31] and 50 nontargeting control sgRNAs were included. sgRNA guide sequences (full list, Table S1) were cloned into lentiCRISPRv2-puro (Addgene #52961) by the Genome Engineering and iPSC core (GEiC) at Washington University. The sgRNA plasmid library was packaged in HEK293T cells with psPAX2 (provided by DidierTrono, Addgene #12260) and pMD2.G (provided by DidierTrono, Addgene #12259) using TurboFectin 8.0 transfection reagent according to manufacturer's instructions. Supernatants were harvested 2 days post-transfection, pooled, clarified by centrifugation (1,200 x rpm for 5 min), filtered through a 0.45 μm membrane, and stored at −80°C.

We transduced 2.4 x 10^7 HAP1 cells at an MOI of 0.1–0.3 with the packaged lentiviral library and selected cells with puromycin (2 μg/mL) for 7–10 days. We then inoculated 5 x 106 cells with SINV-WEEV-GFP McMillan at an MOI of 3. Surviving cells were propagated in the presence of a neutralizing mouse monoclonal antibody (WEEV-209) and re-inoculated after expansion to 5 x 10^6 cells with SINV-WEEV-GFP McMillan. The surviving cells were expanded, and cell pellets frozen at −80°C. gDNA from the control and selected cell pellets were prepared using Monarch Genomic DNA Purification Kit (NEB). The guide sequences were amplified from genomic DNA using a pooled forward primer set (5′-AATGATACGGCGACCACCGAGATCTACACCTGATGACACTCTTTCCCTACACGACGCTCTTCCGATCTN$_{1\text{-}6}$TTGTGGAAAGGACGAAACACCG -3′) and a barcoded reverse primer (5′CAAGCAGAAGACGGCATACGAGATN$_8$GTGACTGGAGTTCAGACGTGTGCTCTTCCGATCTCCAATTCCCACTCCTTTCAAGACCT -3′). The amplified product was purified by gel extraction and subject to (1 x 150bp) sequencing on an Illumina MiSeq instrument. sgRNA sequences were extracted from the demultiplexed FASTQ files, and enriched genes were identified compared to control library cells with the MAGeCK package.[32,33]

Gene validation and ectopic expression—The following sgRNAs: 'TCCTCACTCACCGGTTCCGG' human *VLDLR* and 'AAAACAGGACGATGTGCGGC' as a non-targeting control was cloned into the LentiCRISPR-v2-blast backbone. Lentivirus was generated by transfecting HEK293T cells with the transfer vector, psPAX2, and pMD2.G at a 2:2:1 ratio and harvesting the supernatant after 48 h. HAP1 cells were transduced with lentivirus and subjected to blasticidin selection (10 μg/mL) for 7 days. Selected cells were cloned by limiting dilution. To identify VLDLR-deficient clones, cells were incubated sequentially with anti-VLDLR (5 μg/mL, clone 1H5) and goat anti-mouse-IgG recombinant Fab A647 (1 μg/mL) prior to analysis by flow cytometry.

cDNA encoding *VLDLR* (GenBank NP_003374.3) residues 28–873, mouse *Mxra8*, and chicken *MXRA8* were cloned with an N-terminal FLAG tag into the pLV-IRES-puromycin

or -blasticidin lentiviral vector as described.13 The VLDLRΔLBD construct was cloned by PCR amplification of the residues 373–873 of *VLDLR* and assembly into the pLV-IRES-puro vector with the HiFi DNA assembly kit (NEB). The VLDLRΔcyt construct was generated by deleting resdiues 822–867 from the *VLDLR* construct. The VLDLR-GPI construct was generated by replacing residues 799–873 of the *VLDLR* construct with the following sequence encoding the PLAP GPI anchor: 5′-CCCCCAGCAGGAACAACTGATGCTGCTCATCCTGGTAGGAGTGTTGTCCCCGCGTTGCTTCCTCTGCTGGCCGGGACCCTGCTGCTGCTGGAGACGGCCACTGCTCCCTAG-3’. Lentiviruses were produced as described above and ‘spinoculated’ (800 x g for 25 min) into K562 cells. Transduced cells were selected after 48 h of incubation with puromycin (2 μg/mL, Invivogen) and 7 days of culture before use. To verify expression after selection, cells were incubated with anti-Flag-Alexa Flour 647 (15009S, Cell Signaling) at a 1:200 dilution in FACS buffer (1x PBS +0.1% BSA +2 mM EDTA +0.05% NaN_3) for 30 min at 4°C. Following washing steps, cells were analyzed on an iQue3 flow cytometer (Sartorius) and Forecyt software. For some experiments, cells stained with anti-Flag-A647 were sorted equivalent expression on a MACSQuant Tyto instrument (Miltenyi Biotec).

K562 cells expressing Flag-tagged wild-type or GPI-anchored VLDLR were rinsed twice with PBS and treated with 1 U/ml of phosphatidylinositol-specific phospholipase C (PI-PLC) (Sigma-Aldrich #P8804) in 50 μL of PBS for 2 h at 37°C. After rinsing with twice more with PBS, cells were stained for Flag expression and analyzed by flow cytometry.

Infection experiments—HAP1 cells: Cells were inoculated at an MOI 3 for 8 h prior to analysis. K562 cells: Cells were inoculated at an MOI 3 for 24 h. HEK293T cells: To assess neutralization capacity of Fc-fusion protein, alphaviruses were incubated at 37°C for 1 h prior to inoculation of HEK293T cells. Cells were harvested after 16 h and subjected to flow cytometric analysis using an iQue3 flow cytometer.

Multi-step viral growth analysis—10^6 control or transduced K562 cells were incubated with SINV-WEEV-GFP McMillan, SINV-EEEV-GFP FL93, or RRV-T48-GFP at an MOI of 0.1 in 1 mL of RPMI supplemented with 2% FBS for 2 h at 37°C. Subsequently, unbound virus was removed by three washes in media, and the cells were resuspended in 2 mL of RPMI 10% FBS. Culture supernatant (0.2 mL) was harvested at 2, 6 12, 24, 48 h and replaced with an equivalent volume of fresh media. The supernatant was immediately frozen and subsequently titered on Vero cells by focus-forming assay.

Virus attachment and internalization assays—We generated a high titer stock of SINV-WEEV McMillan through concentration of virus-containing supernatant by ultracentrifugation (150,000 x g, 2 h, SW32Ti) through a 20% sucrose cushion in 50 mM Tris pH 7.4, 100 mM NaCl, 0.1 mM EDTA (TNE) buffer. To assess virus attachment to the cell surface, purified SINV-WEEV-McMillan virus (MOI of 30) was incubated with control or transduced K562 cells on ice for 1 h in complete media. Unbound virus was removed by washing three times with ice-cold binding buffer (Hank’s Balanced Salt Solution [HBSS] supplemented with 2 mM $CaCl_2$, and 2% BSA). Cells were then fixed with 4% paraformaldehyde for 15 min and incubated with 1 μg/mL of anti-WEEV E2 (WEEV-209) for 30 min and 1 μg/mL of anti-mouse-IgG-AF647 secondary antibody prior

to flow cytometry analysis. To assess virus internalization, after removing unbound virus, cells were incubated at 37°C for 1 h to allow for internalization. Cells were resuspended in PBS supplemented with 0.5 mg/mL of proteinase K (Sigma, P2308) for 2 h on ice to digest bound but uninternalized virus. Cells then were fixed with 4% paraformaldehyde and permeabilized with FACS Buffer supplemented with 0.1% saponin. Cells were incubated sequentially for 30 min with 1 μg/mL of WEEV-209 and 1 μg/mL of anti-mouse-IgG-AF647 secondary antibody in perm-wash buffer prior to processing on an iQue flow cytometer.

Fc-fusion protein production—MXRA8-Fc and LDLRAD3-LA1-Fc were produced as described previously.[8,9] The ligand binding domain (LA1–8) of human VLDLR (residues 28–355, GenBank: NP_003374.3) was subcloned into a pTwist CMV β-globin expression vector human IgG1 Fc down-stream of a mouse IgH signal sequence and upstream of human IgG1 separated by a GGGSGGS linker as previously described.[10] To express proteins, constructs were transfected with human LRPAP1 (RAP) chaperone protein (residues 1–353) at a 4:1 ratio with Expifectamine 293 reagent into Expi293 cells (Thermo Fisher) according to the manufacturer's instructions. Supernatants were harvested four days post-transfection, centrifuged (4,000 x g) and passed through a 0.22-μm filter. Fc-fusion proteins were bound to Protein A Sepharose using a gravity flow column. The column was washed with 25 volumes of 1x TBS (20 mM Tris pH 8.0, 150 mM NaCl), 50 column volumes of high-salt buffer (20 mM Tris pH 8.0, 500 mM NaCl, 10 mM EDTA) to strip LRPAP1, followed by 25 volumes of 1x TBS +10 mM $CaCl_2$. Proteins were eluted with Pierce Gentle Ag/Ab Elution Buffer, pH 6.6 (Thermo Fisher) and desalted into 1x TBS (20 mM Tris pH 8.0,150 mM NaCl) with 2 mM $CaCl_2$ using a PD-10 column (Cytiva). Depending on the yield, protein was concentrated with an Amicon 10 kDa centrifugal filter (Millipore). Protein purity was assessed by reducing and non-reducing SDS-PAGE followed by staining with SimpliSafe Coomasie reagent (Thermo Fisher). Gels were imaged with an iBright 1500 instrument (Thermo Fisher).

Cell surface Fc-fusion binding—Vero cells were inoculated (MOI of 5–10) with SINV-WEEV-GFP McMillan, SINV-EEEV-GFP FL93-939, SINV-VEEV-GFP TrD, and SINV-CHIKV-GFP LR in DMEM supplemented with 2% FBS. After allowing infection to proceed for 16 h, cells were detached using TrypLE (Thermo Fisher) and washed with 1x PBS. Cells were incubated with increasing concentrations of VLDLR-LBD-Fc, LDLRAD3-LA1-Fc, mouse MXRA8-Fc or human anti-E1 DC2. 112 mAb for 30 min at 4°C in HBSS containing calcium and magnesium (Thermo Fisher Cat#14025092) supplemented with 0.1% BSA and 0.05% NaN_3 (HBSS-BN). Cells were washed and then incubated with Alexa Fluor 647-conjugated goat anti-human or anti-mouse IgG (1:2000 dilution in HBSS-BN; Thermo Fisher) for 15 min at 4°C. Cells were washed and resuspended in HBSS-BN containing 4′4,6-diamidino-2-phenylindole (DAPI, 1 μg/mL) to stain dead cells and subjected to flow cytometry analysis using an iQue3 flow cytometer (Sartorius).

Virus-like particles (VLPs)—A pCAGGS vector encoding WEEV McMillan structural genes was modified to remove a putative nuclear localization signal in the capsid (K67N, K69N, K82N, K84N, K91N) by Gibson assembly of GeneBlocks (IDT). To generate VLPs, Expi293 cells were transfected using an Expifectamine 293 kit according to

the manufacturer's instructions with the modified pCAGGS construct. The culture was harvested after 72 h and centrifuged (3000 x *g*) for 20 min to remove cells and debris. The supernatant was subjected to PEG precipitation (6% PEG-8000, 600 mM NaCl) overnight at 4°C. Subsequently, the solution was centrifuged (4000 x *g*) for 30 min at 4°C. The pellet was resuspended in TNE buffer and loaded onto a discontinuous sucrose gradient (20% and 60%) followed by ultracentrifugation (170,000 x *g* for 90 min, SW32Ti rotor). The band containing VLPs at the 20%–60% interface was collected and diluted in 1x TBS prior to concentration with an Amicon 100 kDa cutoff filter. VLPs were used immediately for binding experiments or flash-frozen and stored at −80°C. Purity was assessed by non-reducing SDS-PAGE followed by staining with SimpliSafe Coomasie reagent (Thermo Fisher). VEEV TC-83 and CHIKV 37997 VLPs were gifts of John Mascola (Vaccine Research Center, NIH)[34] and Emergent Biosolutions,[35] respectively.

Biolayer interferometry—Binding experiments were performed on a GatorPlus BLI and analyzed using on-board software (GatorBio). Experiments were performed with 1x TBS supplemented with 1% BSA and 2 mM $CaCl_2$ (Running buffer). To evaluate the binding of Fc-fusion receptor proteins in solution, anti-His biosensors (GatorBio) were incubated with 10 μg/mL of recombinantly-designed and produced Histagged versions of mWEEV-251, hVEEV-63,[36] or hCHK-265[37] mAbs followed by capture of WEEV McMillan, VEEV TC-83, or CHIKV 37997 VLPs, respectively. After washing in running buffer for 30 s, the tethered VLPs were incubated with 5 μg/mL of the indicated Fc-fusion proteins for the indicated time and binding signal was recorded. To measure binding affinity, VLP coated biosensors were dipped into monomeric VLDLR fragments cleaved from the Fc fusion protein using Fabdello (Genovis #B1-BD1-008). Steady state (equilibrium) affinity was determined via on-board GatorOne Software (v2.7, GatorBio).

Neutralization studies—To assess the neutralization capacity of Fc-fusion proteins, HEK293T cells were plated (2.5 x 10^4 per well) in a 96-well plate and allowed to adhere overnight in DMEM-10% FBS. The following day, alphaviruses were incubated with Fc-fusion proteins for 1 h at 37°C in DMEM-2%FBS before inoculation of HEK293T (MOI 0.5) cells or K562 cells (MOI 3). Cells were harvested 16 h (HEK293T) or 24 h (K562) post-infection subjected to flow cytometric analysis.

Mouse experiments

Decoy experiments: 10^3 FFU of WEEV McMillan or 10^2 FFU VEEV ZPC738 were mixed with 50 μg of VLDLR LBD-Fc or LDLRAD3-LA1-Fc for 30 min at room temperature before subcutaneous inoculation in the footpad. Mice were administered an additional 100 μg of the appropriate Fc-fusion protein by intraperitoneal injection 1-day post-infection. Mice were monitored daily for survival and weight loss. In separate prophylaxis experiments, mice were given a 200 μg dose of VLDLR LBD-Fc or LDLRAD3-LA1-Fc via intraperitoneal injection at 24 h and 4 h before injection followed by an additional 200 μg dose 24 h after WEEV infection. At 4 days post-innoculation, some mice euthanized, and after extensive perfusion with PBS, tissues were collected and stored at −80°C prior to processing. Subsequently, tissues were homogenized with a MagNA Lyser (Roche), and viral RNA was extracted with a

MagMAX Viral RNA extraction kit using a Kingfisher Flex instrument (Thermo Fisher) according to the manufacturer's instructions. Viral RNA levels were determined using a TaqMan RNA-to-Ct 1-Step Kit on a QuantStudio 6 (Thermo Fisher) using the following primer and probe sets: WEEV-forward 5′-AGATATTGCCCAATCCAGAAA-3′, WEEV-reverse 5' -TATGCGCCTCTGAAGGAAATAG-3′, and WEEV-probe 5'-/56-FAM/AAGCAATTA/ZEN/CAGCGGAGCGACTCA/3IABKFQ/- FFU equivalents were determined by parallel processing of a viral stock with known titer.

Pathogenesis studies: Mice were inoculated subcutaneously with 10^3 FFU of WEEV McMillan, 2 x 10^2 FFU of EEEV-MADV-Argentina-1936, or 10^2 FFU of VEEV ZPC738. 10^3 FFU of SFV Kumba was administered by intraperitoneal injection. Mice were monitored daily for survival and weight loss. At 5 dpi, some cohorts were euthanized, and tissues were processed for viral burden as described above. For intracranial infections, 10^2 FFU of WEEV McMillan in 30 μL was injected into the caudal region of the left cortex using a pre-measured needle guide and a 0.3 mL 29G x % ½" insulin syringe (Exel Int #26018). At 36 h post-infection, mice were euthanized, and perfused. Brains were separated into three regions: cortex, cerebellum, and brainstem. To determine the viral load in harvested tissue, the clarified homogenates were titered on Vero cells by focus-forming assay.

QUANTIFICATION AND STATISTICAL ANALYSIS

Statistical significance was determined using Prism Version 8.0 (GraphPad) when $p < 0.05$. Statistical analysis of viral infection levels was evaluated by one-way ANOVA with Dunnett's post-test. Analysis or mortality was determined by Kaplan-Meier survival curve analysis. The statistical tests, number of independent experiments, and number of experimental replicates are indicated in the Figure legends.

Supplementary Material

Refer to Web version on PubMed Central for supplementary material.

ACKNOWLEDGMENTS

The studies were supported by NIH grants R01 AI141436 (M.S.D.) and R01 AI153209 (W.B.K.), contract AI201800001 (to M.S.D.), U19 AI142790 (to M.S.D. and D.H.F.), R01 AI163019 (S.P.J.W.), T32 AI007172 (to S.P.), and T32 CA009547 (to A.S.); NIAID contract 75N93022C00035 (to D.H.F.); and a Defense Threat Reduction Agency contract MCDC2103-01 (to W.B.K. and M.S.D.). We thank the DNA Sequencing Innovation Lab at The Edison Family Center for Genome Sciences & Systems Biology at Washington University for their assistance with next-generation sequencing and William de Souza for providing the sequence of WEEV EQ1090_2023. The graphical abstract and parts of Figure S1 were generated using BioRender.

REFERENCES

1. Paessler S, Yun NE, Judy BM, Dziuba N, Zacks MA, Grund AH, Frolov I, Campbell GA, Weaver SC, and Estes DM (2007). Alpha-beta T cells provide protection against lethal encephalitis in the murine model of VEEV infection. Virology 367, 307–323. [PubMed: 17610927]
2. Paessler S, Ni H, Petrakova O, Fayzulin RZ, Yun N, Anishchenko M, Weaver SC, and Frolov I (2006). Replication and clearance of Venezuelan equine encephalitis virus from the brains of animals vaccinated with chimeric SIN/VEE viruses. J. Virol 80, 2784–2796. [PubMed: 16501087]

3. Reeves WC, Hutson GA, Bellamy RE, and Scrivani RP (1958). Chronic latent infections of birds with Western equine encephalomyelitis virus. Proc. Soc. Exp. Biol. Med 97, 733–736. [PubMed: 13554464]

4. Deresiewicz RL, Thaler SJ, Hsu L, and Zamani AA (1997). Clinical and Neuroradiographic Manifestations of Eastern Equine Encephalitis. N. Engl. J. Med 336, 1867–1874. [PubMed: 9197215]

5. Weaver SC, and Barrett ADT (2004). Transmission cycles, host range, evolution and emergence of arboviral disease. Nat. Rev. Microbiol 2, 789–801. [PubMed: 15378043]

6. Campos AS, Franco AC, Godinho F, Huff R, da Cruz Cardoso J, Morais P, Franceschina C, de Lima Bermann T, dos Santos FM, Bauermann M, et al. (2024). Molecular epidemiology of Western equine encephalitis virus in Brazil, 2023-2024. Preprint at medRxiv. 10.1101/2024.04.15.24305848.

7. Coates EE, Edupuganti S, Chen GL, Happe M, Strom L, Widge A, Florez MB, Cox JH, Gordon I, Plummer S, et al. (2022). Safety and immunogenicity of a trivalent virus-like particle vaccine against western, eastern, and Venezuelan equine encephalitis viruses: a phase 1, open-label, dose-escalation, randomised clinical trial. Lancet Infect. Dis 22, 1210–1220. [PubMed: 35568049]

8. Zhang R, Kim AS, Fox JM, Nair S, Basore K, Klimstra WB, Rimkunas R, Fong RH, Lin H, Poddar S, et al. (2018). Mxra8 is a receptor for multiple arthritogenic alphaviruses. Nature 557, 570–574. [PubMed: 29769725]

9. Ma H, Kim AS, Kafai NM, Earnest JT, Shah AP, Case JB, Basore K, Gilliland TC, Sun C, Nelson CA, et al. (2020). LDLRAD3 is a receptor for Venezuelan equine encephalitis virus. Nature 588, 308–314. [PubMed: 33208938]

10. Clark LE, Clark SA, Lin C, Liu J, Coscia A, Nabel KG, Yang P, Neel DV, Lee H, Brusic V, et al. (2022). VLDLR and ApoER2 are receptors for multiple alphaviruses. Nature 602, 475–480. [PubMed: 34929721]

11. Zhai X, Li X, Veit M, Wang N, Wang Y, Merits A, Jiang Z, Qin Y, Zhang X, Qi K, et al. (2024). LDLR is used as a cell entry receptor by multiple alphaviruses. Nat. Commun 15, 622. [PubMed: 38245515]

12. Ma H, Adams LJ, Raju S, Sariol A, Kafai NM, Janova H, Klimstra WB, Fremont DH, and Diamond MS (2024). The low-density lipoprotein receptor promotes infection of multiple encephalitic alphaviruses. Nat. Commun 15, 246. [PubMed: 38172096]

13. Zimmerman O, Zimmerman MI, Raju S, Nelson CA, Errico JM, Madden EA, Holmes AC, Hassan AO, VanBlargan LA, Kim AS, et al. (2023). Vertebrate-class-specific binding modes of the alphavirus receptor MXRA8. Cell 186, 4818–4833.e25. [PubMed: 37804831]

14. Adams LJ, Raju S, Ma H, Gilliland T, Reed DS, Klimstra WB, Fremont DH, and Diamond MS (2024). Structural and functional basis of VLDLR usage by Eastern equine encephalitis virus. Cell 187, 360–374.e19. 10.1016/j.cell.2023.11.031. [PubMed: 38176410]

15. Kafai NM, Janova H, Cain MD, Alippe Y, Muraro S, Sariol A, Elam-Noll M, Klein RS, and Diamond MS (2023). Entry receptor LDLRAD3 is required for Venezuelan equine encephalitis virus peripheral infection and neurotropism leading to pathogenesis in mice. Cell Rep. 42, 112946. [PubMed: 37556325]

16. Byrnes AP, and Griffin DE (1998). Binding of Sindbis virus to cell surface heparan sulfate. J. Virol 72, 7349–7356. [PubMed: 9696831]

17. Zhang W, Heil M, Kuhn RJ, and Baker TS (2005). Heparin binding sites on Ross River virus revealed by electron cryo-microscopy. Virology 332, 511–518. [PubMed: 15680416]

18. Chen C-L, Hasan SS, Klose T, Sun Y, Buda G, Sun C, Klimstra WB, and Rossmann MG (2020). Cryo-EM structure of eastern equine encephalitis virus in complex with heparan sulfate analogues. Proc. Natl. Acad. Sci. USA 117, 8890–8899. [PubMed: 32245806]

19. Tanaka A, Tumkosit U, Nakamura S, Motooka D, Kishishita N, Priengprom T, Sa-Ngasang A, Kinoshita T, Takeda N, and Maeda Y (2017). Genome-wide screening uncovers the significance of N-sulfation of heparan sulfate as a host cell factor for Chikungunya virus infection. J. Virol 91, e00432–17. 10.1128/JVI.00432-17. [PubMed: 28404855]

20. Gardner CL, Choi-Nurvitadhi J, Sun C, Bayer A, Hritz J, Ryman KD, and Klimstra WB (2013). Natural variation in the heparan sulfate binding domain of the eastern equine encephalitis virus E2

glycoprotein alters interactions with cell surfaces and virulence in mice. J. Virol 87, 8582–8590. [PubMed: 23720725]

21. Li W, Plante JA, Lin C, Basu H, Plung JS, Fan X, Boeckers JM, Oros J, Buck TK, Anekal PV, et al. (2024). Shifts in receptors during submergence of an encephalitic arbovirus. Nature 632, 614–621. [PubMed: 39048821]
22. Salimi H, Cain MD, Jiang X, Roth RA, Beatty WL, Sun C, Klimstra WB, Hou J, and Klein RS (2020). Encephalitic Alphaviruses Exploit Caveola-Mediated Transcytosis at the Blood-Brain Barrier for Central Nervous System Entry. mBio 11, e02731–19. 10.1128/mBio.02731-19. [PubMed: 32047126]
23. Anishchenko M, Paessler S, Greene IP, Aguilar PV, Carrara A-S, and Weaver SC (2004). Generation and characterization of closely related epizootic and enzootic infectious cDNA clones for studying interferon sensitivity and emergence mechanisms of Venezuelan equine encephalitis virus. J. Virol 78, 1–8. [PubMed: 14671082]
24. Gardner CL, Sun C, Dunn MD, Gilliland TC Jr., Trobaugh DW, Terada Y, Reed DS, Hartman AL, and Klimstra WB (2022). In vitro and in vivo phenotypes of Venezuelan, eastern and western equine encephalitis viruses derived from cDNA clones of human isolates. Viruses 15, 5. [PubMed: 36680046]
25. Sun C, Gardner CL, Watson AM, Ryman KD, and Klimstra WB (2014). Stable, high-level expression of reporter proteins from improved alphavirus expression vectors to track replication and dissemination during encephalitic and arthritogenic disease. J. Virol 88, 2035–2046. [PubMed: 24307590]
26. Kuhn RJ, Niesters HG, Hong Z, and Strauss JH (1991). Infectious RNA transcripts from Ross River virus cDNA clones and the construction and characterization of defined chimeras with Sindbis virus. Virology 182, 430–441. [PubMed: 1673812]
27. Morrison TE, Whitmore AC, Shabman RS, Lidbury BA, Mahalingam S, and Heise MT (2006). Characterization of Ross River virus tropism and virus-induced inflammation in a mouse model of viral arthritis and myositis. J. Virol 80, 737–749. [PubMed: 16378976]
28. Sievers F, Wilm A, Dineen D, Gibson TJ, Karplus K, Li W, Lopez R, McWilliam H, Remmert M, Söding J, et al. (2011). Fast, scalable generation of high-quality protein multiple sequence alignments using Clustal Omega. Mol. Syst. Biol 7, 539. [PubMed: 21988835]
29. Yu G, Smith DK, Zhu H, Guan Y, and Lam TT-Y (2017). Ggtree: An r package for visualization and annotation of phylogenetic trees with their covariates and other associated data. Methods Ecol. Evol 8, 28–36.
30. Song J, Chow RD, Peña-Hernández MA, Zhang L, Loeb SA, So E-Y, Liang OD, Ren P, Chen S, Wilen CB, and Lee S (2022). LRRC15 inhibits SARS-CoV-2 cellular entry in trans. PLoS Biol. 20, e3001805. [PubMed: 36228039]
31. Sanson KR, Hanna RE, Hegde M, Donovan KF, Strand C, Sullender ME, Vaimberg EW, Goodale A, Root DE, Piccioni F, and Doench JG (2018). Optimized libraries for CRISPR-Cas9 genetic screens with multiple modalities. Nat. Commun 9, 5416. [PubMed: 30575746]
32. Li W, Xu H, Xiao T, Cong L, Love MI, Zhang F, Irizarry RA, Liu JS, Brown M, and Liu XS (2014). MAGeCK enables robust identification of essential genes from genome-scale CRISPR/Cas9 knockout screens. Genome Biol. 15, 554. [PubMed: 25476604]
33. Li W, Köster J, Xu H, Chen C-H, Xiao T, Liu JS, Brown M, and Liu XS (2015). Quality control, modeling, and visualization of CRISPR screens with MAGeCK-VISPR. Genome Biol. 16, 281. [PubMed: 26673418]
34. Ko S-Y, Akahata W, Yang ES, Kong W-P, Burke CW, Honnold SP, Nichols DK, Huang Y-JS, Schieber GL, Carlton K, et al. (2019). A virus-like particle vaccine prevents equine encephalitis virus infection in nonhuman primates. Sci. Transl. Med 11, eaav3113. 10.1126/scitranslmed.aav3113. [PubMed: 31092692]
35. Raju S, Adams LJ, Earnest JT, Warfield K, Vang L, Crowe JE Jr., Fremont DH, and Diamond MS (2023). A chikungunya virus-like particle vaccine induces broadly neutralizing and protective antibodies against alphaviruses in humans. Sci. Transl. Med 15, eade8273. [PubMed: 37196061]
36. Kafai NM, Williamson LE, Binshtein E, Sukupolvi-Petty S, Gardner CL, Liu J, Mackin S, Kim AS, Kose N, Carnahan RH, et al. (2022). Neutralizing antibodies protect mice against Venezuelan

equine encephalitis virus aerosol challenge. J. Exp. Med 219, e20212532. 10.1084/jem.20212532. [PubMed: 35297953]

37. Fox JM, Long F, Edeling MA, Lin H, van Duijl-Richter MKS, Fong RH, Kahle KM, Smit JM, Jin J, Simmons G, et al. (2015). Broadly Neutralizing Alphavirus Antibodies Bind an Epitope on E2 and Inhibit Entry and Egress. Cell 163, 1095–1107. [PubMed: 26553503]
38. Quiroz JA, Malonis RJ, Thackray LB, Cohen CA, Pallesen J, Jangra RK, Brown RS, Hofmann D, Holtsberg FW, Shulenin S, et al. (2019). Human monoclonal antibodies against chikungunya virus target multiple distinct epitopes in the E1 and E2 glycoproteins. PLoS Pathog. 15, e1008061. [PubMed: 31697791]

Highlights

- VLDLR is a receptor for several WEEV strains
- Soluble VLDLR decoy neutralizes WEEV infection *in vitro* and *in vivo*
- VLDLR KO mice survive lethal challenge by WEEV, SFV, and EEEV-MADV but not VEEV
- VLDLR KO mice have decreased virus in the brain after intracranial WEEV infection

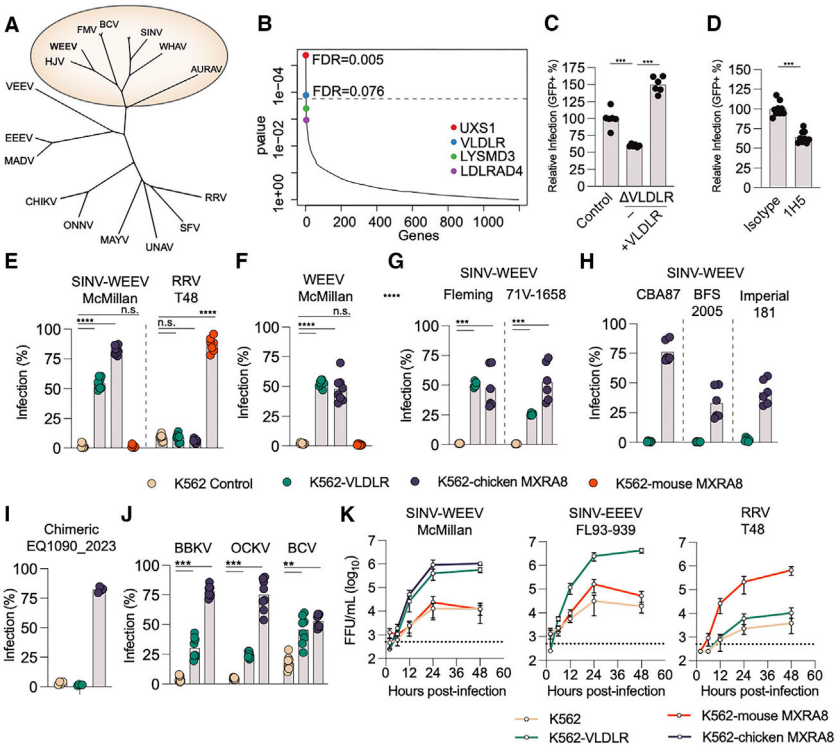

Figure 1. A CRISPR-Cas9 screen identifies VLDLR as a factor that promotes WEEV infection

(A) Phylogenetic tree generated from structural protein sequences of indicated alphaviruses with members of the WEE complex highlighted in brown.

(B) MAGeCK plot of enriched genes in surviving cells following two rounds of SINV-WEEV-GFP infection.

(C) SINV-WEEV-GFP McMillan infection (MOI of 3, 8 h) in HAP-1 control, *ΔVLDLR*, and *ΔVLDLR* complemented with VLDLR-FLAG cells as assessed by GFP expression (pooled from 3 experiments performed in triplicate; all data points are shown).

(D) SINV-WEEV-GFP McMillan infection in HAP-1 cells pre-treated with blocking anti-VLDLR antibody (1H5) for 1 h prior (pooled from 2–3 experiments performed in duplicate or triplicate; all data points are shown).

(E–J) Infection of indicated viruses (MOI of 3, 24 h) as quantified by GFP expression (E, G, and H), WEEV-209 mAb (anti-WEEV E2) staining (F, H, and I), or DC2.112[38] (pan alphavirus anti-E1) staining (J) of K562 control, K562-VLDLR, K562-chicken MXRA8, or K562-mouse MXRA8 cells (pooled from 3–4 independent experiments performed in duplicate; all data points are shown).

(K) Viral growth curves in the indicated cell lines after inoculation with SINV-WEEV McMillan, SINV-EEEV FL93, and RRV T48 (MOI of 0.1) as determined by focus-forming assay on Vero cells (pooled from 4 experiments; error bars indicate standard error of the mean).

Dotted lines show the limit of detection (LOD), and column heights indicate mean values. Statistical analysis was performed on the mean values of the biological replicates: (C and E–H) one-way ANOVA with Tukey's post-test and (D) Student's t test (ns, not significant, $^{**}p < 0.01$, $^{***}p < 0.001$, and $^{****}p < 0.0001$).

See also Figures S1 and S2 and Tables S1 and S2.

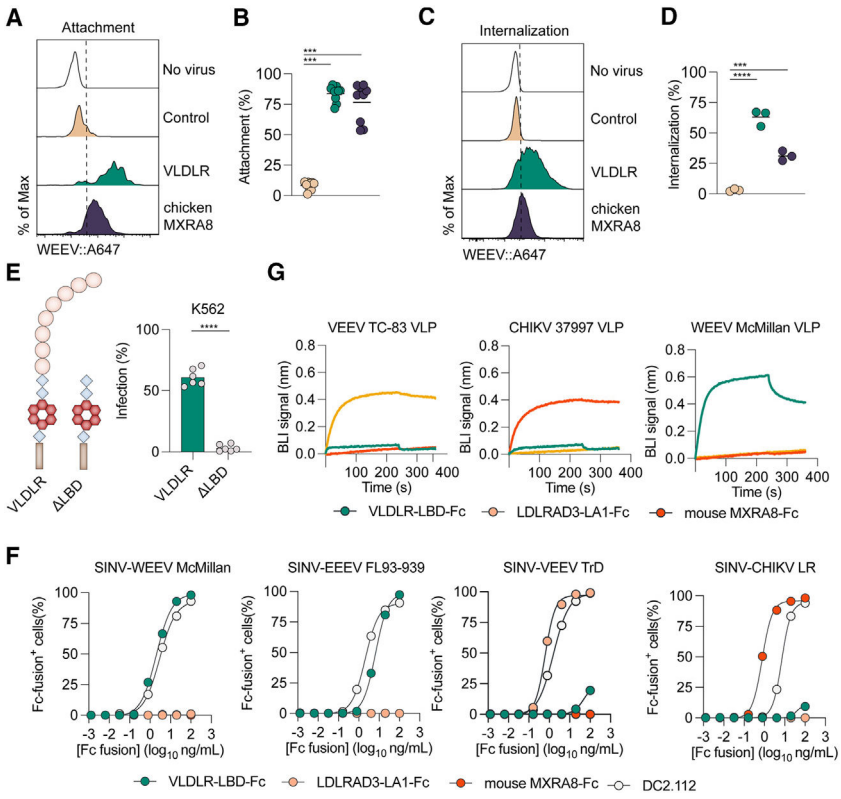

Figure 2. VLDLR promotes attachment and internalization of WEEV via its ligand-binding domain

(A and B) Attachment of SINV-WEEV to the cell surface. Flow cytometry plots (A) and quantification (B) of anti-E2 (WEEV-209) staining of the surface of K562-, K562-chicken MXRA8-, and K562-VLDLR-expressing cells following incubation with SINV-WEEV at 4°C (pooled from 3 experiments performed in triplicate; all data points are shown).

(C and D) Internalization of SINV-WEEV by cells. Flow cytometry plots (C) and quantification (D) of intracellular E2 (anti-WEEV-209) staining of K562-, K562- chicken MXRA8-, and K562-VLDLR-expressing cells following incubation with SINV-WEEV at 37°C (pooled from 3 experiments performed in triplicate).

(E) Diagram of VLDLR and VLDLRΔLBD proteins (left); infection as assessed by GFP expression by flow cytometry (right) of K562 cells expressing VLDLR or VLDLRΔLBD after inoculation (MOI 3, 24 h) with SINV-WEEV-GFP McMillan (pooled from 3 experiments in duplicate).

(F) Quantification of cell surface binding by indicated concentration of Fc-fusion proteins to Vero cells inoculated with indicated chimeric SINV (pooled from 2 experiments).

(G) Binding of Fc-fusion proteins to immobilized VLPs. The indicated VLPs were captured on biosensors using mouse mAbs followed by incubation with 5 μg/mL of indicated Fc-fusion proteins (representative of two experiments).

Column heights and bars indicate mean values. Statistical analysis was performed on the mean values of the biological replicates: (B and D) one-way ANOVA with Tukey's post-test and (E) Student's t test (***$p < 0.001$ and ****$p < 0.0001$).

See also Figures S2 and S3.

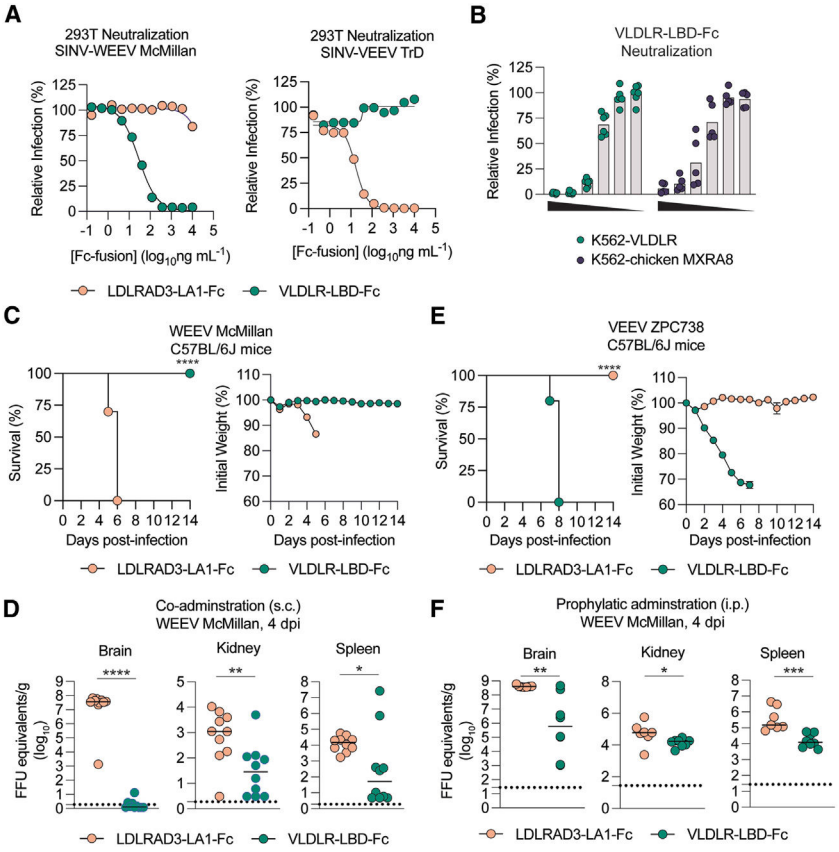

Figure 3. VLDLR-LBD-Fc neutralizes WEEV McMillan infection and protects against lethal challenge

(A) SINV-WEEV-GFP McMillan and SINV-VEEV-GFP TrD infection as assessed by GFP expression following incubation with indicated soluble receptor decoy proteins prior to inoculation of HEK293T cells. Data are normalized to infection with no protein (pooled from 3 experiments).

(B) SINV-WEEV-GFP McMillan infection following incubation with indicated decoy proteins (10 μg/mL, 3-fold dilutions) prior to inoculation of the indicated K562 cells (pooled from 3 experiments performed in duplicate; all data points are shown).

(C and E) Survival (left) and weight loss (right) of 6-week-old C57BL6/J mice injected with VLDLR-LBD-Fc ($n = 10$, C and E) or LDLRAD3-LA1-Fc ($n = 10$, C and E) and 10^3 FFUs of WEEV McMillan (C) or 10^2 FFUs of VEEV ZPC738 (E).

(D and F) Viral RNA levels in indicated tissues at 4 days post-infection (dpi) in mice inoculated with WEEV McMillan and co-administered (D: $n = 10$ for both groups) or administered separately as prophylaxis via an intraperitoneal injection (F: $n = 8$, VLDLR-LBD-Fc; $n = 7$; LDLRAD3-LA1-Fc) the indicated Fc-fusion protein (dotted lines show the limit of detection [LOD]; values at the LOD are plotted slightly below).

Column heights indicate mean values, and bars indicate median values. Statistical analysis: (C and E) log-rank test and (D) Mann-Whitney test (*$p < 0.05$, **$p < 0.01$, and ****$p < 0.0001$).

See also Figure S4.

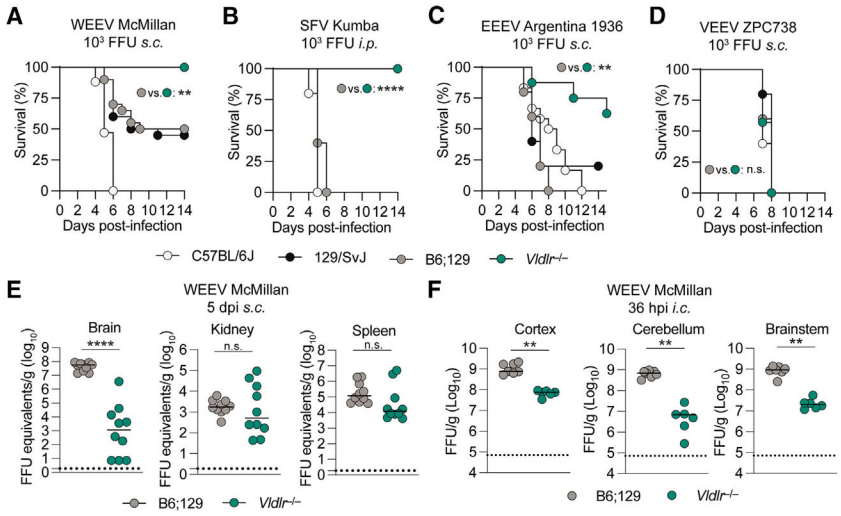

Figure 4. VLDLR-deficient mice are protected from challenge with WEEV and other encephalitic alphaviruses that bind VLDLR

(A–D) Survival rates of indicated mice following subcutaneous inoculation with 10^3 FFUs of WEEV McMillan (A), intraperitoneal inoculation with 10^3 FFUs of SFV Kumba (B), subcutaneous inoculation with 2×10^2 FFUs of EEEV-MADV Argentina 1936 (C), or subcutaneous inoculation with 10^2 FFUs of VEEV ZPC738 (D).

(E) Viral RNA levels as determined by RT-qPCR in the indicated perfused tissues at 5 dpi in mice inoculated subcutaneously with WEEV McMillan.

(F) Viral burden as assessed by focus-forming assay in homogenates of the indicated brain regions at 36 h after intracranial infection of indicated mice with 10^2 FFUs of WEEV McMillan.

Dotted lines show the LOD, and bars indicate median values. Data are pooled from two experiments for each panel as follows (A) $n = 13–20$ per group, (B) $n = 6–7$ per group, (C) $n = 5–8$ per group, (D) $n = 5–7$ per group, (E) $n = 10$ per group, and (F) $n = 7–8$ per group. Statistical analysis: (A–D) log-rank test and (E and F) Mann-Whitney test (ns, not significant, $*p < 0.05$, $**p < 0.01$, and $****p < 0.0001$).

See also Figures S4 and S5.

KEY RESOURCES TABLE

REAGENT or RESOURCE	SOURCE
Antibodies	
WEEV-209	This study
WEEV-231-His	This study
CHK-265	BioXCell
mVEEV-57	BioXCell
DC2.112	Quiroz et al., 2019.[38]
Peroxidase conjugated goat anti-mouse IgG (H + L)	Jackson ImmunoResearc
DYKDDDDK Tag (D6W5B) Rabbit mAb	CST
anti-VLDLR 1H5	Genetex
goat anti-mouse-IgG recombinant Fab A647	Jackson ImmunoResearc
Anti-rabbit IgG (H + L), $F(ab')_2$ Fragment	CST
Peroxidase conjugated goat anti-human IgG (H + L)	Jackson ImmunoResearc
Bacterial and virus strains	
Western equine encephalitis virus (strain McMillan)	Salimi et al.[22]
Venezuelan equine encephalitis virus (strain ZPC738)	Anishchenko et al.[23]
Semliki Forest Virus (strain Kumba)	World Referenc Center for Emerging Viruses and Arboviruses
Madariaga virus (South American EEEV) (strain Argentina 1936)	World Referenc Center for Emerging Viruses and Arboviruses
Babanki virus (strain DAK ArY 251)	World Referenc Center for Emerging Viruses and Arboviruses
Ockelbo virus (strain EDS 14)	World Referenc Center for Emerging Viruses and Arboviruses
Buggy Creek virus (strain 84S217)	World Referenc Center for Emerging Viruses and Arboviruses
Sindbis (strain Girdwood)	Gift from Mark Heise
SINV-WEEV-GFP McMillan	Sun et al.[25]

REAGENT or RESOURCE	SOURCE
SINV-WEEV McMillan	This study
SINV-WEEV-GFP Fleming	This study
SINV-WEEV-GFP BFS2005	This study
SINV-WEEV-GFP Imperial 181	This study
SINV-WEEV-GFP CBA87	Ma et al.[9]
SINV-WEEV-GFP 71V1658	This study
SINV-WEEV-GFP EQ1090_2023	This study
Ross River Virus T48-GFP	Kuhn et al.[26]
SINV-VEEV-GFP TrD	Ma et al.[9]
SINV-CHIKV-GFP LR	Sun et al.[25]
Critical commercial assays	
MagMAX-96 Viral RNA Isolation Kit	Applied Biosystems
Taqman RNA-to-Ct 1-Step Kit	ThermoFisher
Chemicals, peptides, and recombinant proteins	
VLDLR-LBD-Fc	This study; Adam et al.,[14] Raju et al.[35]
LDLRAD3-D1-Fc	This study; Ma al.[9]
mouse MXRA8-Fc	This study
Phosphatidylinositol-specific phospholipase	Sigma-Aldrich
CHIKV 37997 VLPs	Emergent Biosciences
VEEV TC-83 VLP	Ko et al.[34]
WEEV McMillan VLP	This study
Experimental models: Cell lines	
HEK 293T	ATCC
Expi293F	Thermo Fisher
Vero	ATCC
BHK-21	ATCC
HAP1	Horizon Discovery
Experimental models: Organisms/strains	
C57BL/6J	The Jackson Laboratory
129S1/SvImJ	The Jackson Laboratory
B6129SF2/J	The Jackson Laboratory
Vldlr$^{-/-}$	The Jackson Laboratory
Oligonucleotides	

REAGENT or RESOURCE	SOURCE
WEEV *nsP3* forward: 5′- AGATATTGCCCAATCCAGAAA -3′	IDT PrimeTime Assay
WEEV *nsP3* reverse: 5'- TATGCGCCTCTGAAGGAAATAG -3′	IDT PrimeTime Assay
WEEV *nsP3* probe: 5′-/56-FAM/AAGCAATTA/ZEN/CAGCGGAGCGACTCA/3IABKFQ/-3′	IDT PrimeTime Assay
lentiCRISPRv2.FOR: 5′-AATGATACGGCGACCACCGAGATCTACACCTGATGACACTCTTTCCCTACACGACGCTCTTCCGATCTN$_{1-6}$TTGTGGAAAGGACGAAACACCG-3′	IDT Ultramer
lentiCRISPRv2.REV: 5'-CAAGCAGAAGACGGCATACGAGATN$_8$GTGACTGGAGTTCAGACGTGTGCTCTTCCGATCTCCAATTCCCACTCCTTTCAAGACCT-3′	IDT Ultramer
Recombinant DNA	
pLV-FLAG-VLDLR-IRES-puro	This study
pLV-FLAG-VLDLRΔLBD-IRES-puro	This study
pLV-FLAG-VLDLRΔcyt-IRES-puro	This study
pLV-FLAG-VLDLR-GPI-IRES-puro	This study
pLV-FLAG-mouseMxra8-IRES-blast	Zhang et al.[8]
pLV-FLAG-chickenMxra8-IRES-blast	Zimmerman et al.[13]
pCAGGS-WEEV-McMillan VLP	This study
Software and algorithms	
FlowJo	BD Life Science
GraphPad Prism	GraphPad
BioRender	BioRender
Other	
TrypLE	Thermo Fisher